IEEE Access
Multidisciplinary | Rapid Review | Open Access Journal

Received June 2, 2019, accepted June 18, 2019, date of publication June 27, 2019, date of current version July 15, 2019.

Digital Object Identifier 10.1109/ACCESS.2019.2925314

Outage Performance of NOMA-Based Cognitive Hybrid Satellite-Terrestrial Overlay Networks by Amplify-and-Forward Protocols

XIAOKAI ZHANG[1], (Student Member, IEEE), BANGNING ZHANG[1], (Member, IEEE), KANG AN[2], ZHUYUN CHEN[1], (Student Member, IEEE), SILIN XIE[1], HENG WANG[1], LONG WANG[2], AND DAOXING GUO[1], (Member, IEEE)

[1]College of Communications Engineering, PLA Army Engineering University, Nanjing 210007, China
[2]Sixty-Third Research Institute, National University of Defense Technology, Nanjing 210007, China

Corresponding author: Daoxing Guo (xyzgfg@163.com)

ABSTRACT In this paper, we investigate the outage probability (OP) performance of amplify-and-forward (AF) cognitive hybrid satellite-terrestrial overlay networks (CHSTONs) with the non-orthogonal multiple access (NOMA) scheme, in which half-duplexing terrestrial secondary networks cooperate with a primary satellite network for dynamic spectrum access. In order to improve the fairness of overlay paradigm, a NOMA-based power allocation profile is determined by instantaneous channel conditions. Considering the generalized shadowed-Rician fading for satellite links and Nakagami-*m* fading for terrestrial links, we derive the closed-form OP expressions for both the primary and secondary users. Then, the asymptotic OP expressions at the high signal-to-noise ratio (SNR) regime are also obtained to evaluate the achievable diversity order and coding gain. Finally, the numerical simulations are provided to validate the theoretical results as well as the superiority of the NOMA scheme in CHSTONs and proclaim the effect of key parameters on the performance of the NOMA users, such as fading configurations and the power split factor.

INDEX TERMS Non-orthogonal multiple access (NOMA), cognitive hybrid satellite-terrestrial overlay networks (CHSTONs), outage probability.

I. INTRODUCTION

THE line-of-sight satellite communication systems are vulnerable to be blocked by heavy shadowing or obstacles [1]. To resolve this problem, a hybrid satellite-terrestrial system has been proposed [2]–[6], which deploys a terrestrial relay to enhance coverage and high data rate services. Owing to the spectrum scarcity problem, the cognitive radio (CR) of the satellite is proposed to improve the wireless spectrum utilization. Most of researches about cognitive hybrid satellite-terrestrial systems consider the underlay paradigm [7], [8], which allows the secondary users' spectrum access opportunities strictly under the tolerable interference level of the primary user. The interference coordination between the primary and secondary network is one of the key problems to guarantee the quality of service (QoS) of the primary network for underlay paradigm. Another promising CR spectrum sharing paradigm is known to be overlay [9], which means that the secondary users assist the primary transmission through cooperative relaying techniques in exchange for spectrum access. So far, there exists limited works studying the performance of overlay paradigm in hybrid satellite-terrestrial networks. In [10], the authors analyzed the performance of an overlay CR architecture in hybrid satellite-terrestrial networks. One of the assumptions is that the primary co-channel interference can be successfully canceled using its copy received in the first temporal phase, which is arduous in practical scenarios because of the receive capability of the secondary user or dynamic channel conditions. As noted in the paper, the performance of both primary and secondary user would be severely degraded when the decoding of the primary signal is unsuccessful.

Non-orthogonal multiple access (NOMA), utilizing power domain multiplexing, has received increasing research attention by its high spectral efficiency [11]–[16]. Each user transmits signals simultaneously in the same resource block

The associate editor coordinating the review of this manuscript and approving it for publication was Nan Wu.

(i.e., time/frequency) with successive interference cancellation (SIC) employed at receivers to separate the multiplexed signals. Recently, [17]–[23] incorporated the NOMA scheme into satellite networks to improve spectral efficiency. In addition, the NOMA scheme has been introduced into hybrid satellite-terrestrial networks [24]–[26]. The authors in [24] incorporated the beamforming (BF) scheme into satellite-terrestrial integrated networks, where the NOMA was applied among terrestrial users. A cooperative NOMA scheme was proposed [25], in which a user with better channel condition acted as a relay node and forwarded information to other users. The authors in [26] considered a relay node to retransmit the NOMA signal from the satellite in the downlink scenario, and derived the closed-form outage probability (OP) expressions to validate the effectiveness of proposed system model. In order to further improve the spectral utilization efficiency, CR-inspired NOMA scenarios are mainly investigated in terrestrial networks [27]–[30]. The work in [27] investigated the integration of NOMA with CR into holistic 5G system, which constituted a cognitive NOMA network, for more intelligent spectrum sharing. Three different cognitive NOMA architectures were presented, including underlay NOMA networks, overlay NOMA networks, and CR-inspired NOMA networks. Allowing the secondary users and primary users operating simultaneously in a cognitive relay network, [28], [29] introduced NOMA in overlay paradigm into terrestrial communications. However, they only considered the priority of primary user without considering the fairness between the primary network and the secondary network. Without considering the fairness in overlay networks, the secondary relay has no willingness to cooperate with the primary networks.

To our best knowledge, no prior work has analyzed the performance of NOMA in cognitive hybrid satellite-terrestrial overlay networks (CHSTONs) for dynamic power allocation by statistical channel conditions. In addition, the combination of NOMA, CR and hybrid satellite-terrestrial networks framework has a promising potential to allow more nodes (i.e., more secondary users and/or more primary users) and bigger coverage area to transmit concurrently, and thus, can meet the requirements of high spectrum efficiency, massive connectivity, low latency and full coverage for future 6G networks [31].

Inspired by the above observations, a NOMA scheme for CHSTONs is proposed to tackle the fairness issue, cancel the co-channel interference, and improve the spectral efficiency. One of the possible scenarios for the proposed CHSTONs may correspond to DVB-SH service between primary GEO satellite system and secondary TV transmitter-receiver pairs incentivizing through relay cooperation [32], [33].

With the aforementioned CHSTONs configuration, we conduct a comprehensive OP performance analysis for both primary and secondary networks by adopting Shadowed-Rician fading for satellite links and Nakagami-m fading for terrestrial links. The main contributions of this paper are summarized as follows:

- In order to solve the terrestrial spectrum scarcity, enhance the satellite communication coverage and stability, and improve the spectral efficiency, we first introduce the NOMA into CHSTONs. The NOMA power allocation profile is determined by instantaneous channel conditions to improve the fairness of overlay paradigm. Furthermore, the secondary cooperative relay adopts amplify-and-forward (AF) protocols, which reduce the implementation complexity and enhance the security of the satellite transmitted information (i.e. the secondary networks do not decode and get the information from the primary network).
- The signal-to-interference-plus-noise ratio (SINR) of the primary user and the secondary user is formulated in proposed system model. Then, we derive closed-form OP expressions for both the primary and secondary users in CHSTONs. In addition, asymptotic OP expressions at the high signal-to-noise ratio SNR) regime are obtained to evaluate the achievable diversity order and the coding gain.
- We introduce the superiority of the NOMA scheme than traditional OMA, i.e., TDMA. Furthermore, we analyze the effect of key parameters on the OP performance of CHSTONs.

The rest of this paper is organized as follows. Section II introduces the system model of CHSTONs, reformulates SINR, and gives channels fading model. In Section III, the exact and asymptotic OP expressions are derived. Section IV shows simulation results. Finally, conclusions are drawn in Section V.

II. PROBLEM STATEMENT

A. SYSTEM MODEL

An overlay CR diagram of the hybrid satellite-terrestrial network is considered as illustrated in Fig. 1. This scenario comprises a primary satellite transmitter (S), a primary terrestrial user (D), a CR overlay relay (R) and a cognitive user (C). It is worthy to notice that the cognitive user can be multi-users to improve the spectrum efficiency. But, there are several implementation challenges in the NOMA scheme, like error propagation, channel estimation error. Hence, we choose one primary user and one secondary user to apply in a more practical scenario. Due to the heavy shadowing and obstacles, it is difficult to maintain a reliable direct communication (DC) link between S and D. Therefore, the primary satellite has to recruit a secondary transmitter as a relay. In return, the primary networks authorize secondary transmitter spectrum access opportunities. H_{XY} denotes the channel between X and Y, where X, Y could be S, R, D, and C respectively. If the satellite S chooses R as a relay, it indicates that H_{SR} is always better than H_{SD}. Due to promising the assistance of the primary satellite communication, the relay chooses AF protocols in this paper, which reduce the implementation complexity and enhance the security of the satellite transmitted information. In addition, a NOMA scheme is deployed to handle a dilemma of fairness for the relay

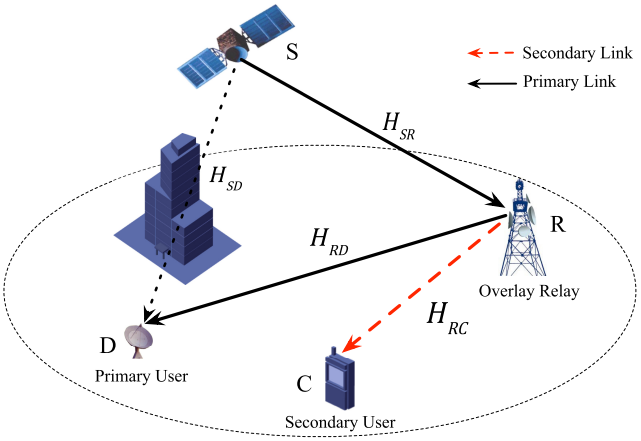

FIGURE 1. Overlay cognitive relay system model.

to allocate the transmitting power. To improve fairness of NOMA schemes [16], more power is allocated to the user with worse channel condition, which is called the weak user.

In the considered system, each node has a single antenna, working in a half-duplex mode (which means that the node cannot transmit and receive simultaneously). Therefore, the overall communication divides into two temporal phases. The satellite sends the signal to the cognitive relay in the first temporal phase, which can be expressed as

$$y_{SR} = \sqrt{P_S} H_{SR} x_p + n_0, \tag{1}$$

where P_S is the satellite transmitter power, and n_0 is the additive white Gaussian noise (AWGN) with mean zero and variance δ_0^2, x_p denotes the signal for satellite transmitter, where $E\left[|x_p|^2\right] = 1$, and $E[\cdot]$ means the expectation operation. The relay transmits mixed superposition signals for both terrestrial user and cognitive receiver. In order to implement NOMA power allocation profile, the channel state information (CSI) parameters should be obtained in overlay relay by a control channel. Much attention has been paid to this kind of channels, some examples are the cognitive pilot channel (CPC) proposed by the E2R2/E3 consortium [34], or the radio enabler proposed by the P1900.4 Working Group [35]. We assume all channels follow quasi-static fading, i.e. the channel gains remain to be constant within each transmission block but vary independently between different blocks. Without loss of generality, it is assumed that two users' relative value of channel gains in the second temporal phase are uncertain, i.e. two kind of situations. For AF protocols, if the secondary link channel conditions are better than the primary's, we have

$$y_{Rm} = \sqrt{\alpha P_R} \frac{H_{Rm} y_{SR}}{\sqrt{|y_{SR}|^2}} + \sqrt{(1-\alpha) P_R} H_{Rm} x_s + n_{1,m}, \tag{2}$$

where $m \in \{D, C\}$, P_R is the relay transmitter power, $n_{1,m}$ is the AWGN with mean zero and variance δ_1^2 or δ_2^2, $\alpha \in (0.5, 1)$ is the power allocation factor, which means that the weak user is allocated more power to improve the fairness, x_s denotes the secondary signal, where $E\left[|x_s|^2\right] = 1$. Owing to the serious fading of H_{SD}, we assume that the primary user would not receive the satellite signal to reduce the meaningless energy consumption in the first temporal phase. According to NOMA, the secondary receiver needs to apply SIC to separate the multiplexed signal. If the primary channel condition is better than the secondary's, we have

$$y_{Rn} = \sqrt{\alpha P_R} H_{Rn} x_s + \sqrt{(1-\alpha) P_R} \frac{H_{Rn} y_{SR}}{\sqrt{|y_{SR}|^2}} + n_{2,n}, \tag{3}$$

where $n \in \{D, C\}$, $n_{2,n}$ is the AWGN with mean zero and variance δ_1^2 or δ_2^2, and the SIC would be conducted in the primary receiver.

B. SINR FORMULATION

We consider an independent but non-identically distributed (i.n.i.d.) channel fading in each temporal phase. The average SNR of each channel is denoted as $\bar{\gamma}_{SR} = \bar{\gamma}_0 = P_S/\delta_0^2$, $\bar{\gamma}_{RD} = \bar{\gamma}_1 = P_R/\delta_1^2$ and $\bar{\gamma}_{RC} = \bar{\gamma}_2 = P_R/\delta_2^2$ respectively. A light shadowing between the satellite and the relay is assumed, which indicates the first temporal phase is relatively reliable. The instantaneous SNR is $\bar{\gamma}_{XY}\rho_{XY}$, where ρ_{XY} denotes $|H_{XY}|^2$. For simplicity, $\rho_{SR} = \rho_0$, $\rho_{RD} = \rho_1$, and $\rho_{RC} = \rho_2$. A NOMA assisted overlay spectrum sharing framework is designed in the second temporal phase, where the primary and secondary messages are superimposed by using the NOMA principle for communications. Since block channel gains are block time-varying, signal detection with SIC should follow the order by instantaneous channel gain. Due to apply the statistical channel model in the OP analysis with concerning both large-scale fading and small-scale fading, we must take two kinds of situations into consideration for long term statistical perspective. For AF protocols, if the primary receiver is the weak user, i.e., $\bar{\gamma}_1\rho_1 \leq \bar{\gamma}_2\rho_2$, the SINR of primary user can be given by

$$\gamma_{1,D} = \frac{\alpha \bar{\gamma}_0 \rho_0 \bar{\gamma}_1 \rho_1}{(1-\alpha)\bar{\gamma}_0\rho_0\bar{\gamma}_1\rho_1 + \bar{\gamma}_0\rho_0 + \bar{\gamma}_1\rho_1 + 1}. \tag{4}$$

Meanwhile, the strong user first decodes the signal of the weak user according to the principle of SIC before detecting its own signal. The decoding SINR is given by

$$\gamma_{C\to D} = \frac{\alpha \bar{\gamma}_2 \rho_2 \bar{\gamma}_0 \rho_0}{(1-\alpha)\bar{\gamma}_2\rho_2\bar{\gamma}_0\rho_0 + \bar{\gamma}_0\rho_0 + \bar{\gamma}_2\rho_2 + 1}. \tag{5}$$

Therefore, $\gamma_{C\to D} > \gamma_{1,D}$, which indicates that a perfect SIC can be conducted. In this regard, the SINR of the strong receiver is

$$\gamma_{1,C} = \frac{(1-\alpha)\bar{\gamma}_2\rho_2(\bar{\gamma}_0\rho_0 + 1)}{\alpha\bar{\gamma}_2\rho_2 + \bar{\gamma}_0\rho_0 + 1}. \tag{6}$$

When $\bar{\gamma}_1\rho_1 > \bar{\gamma}_2\rho_2$, the weak user is the secondary user, the SINR of secondary is given as

$$\gamma_{2,C} = \frac{\alpha\bar{\gamma}_2\rho_2(\bar{\gamma}_0\rho_0 + 1)}{(1-\alpha)(\bar{\gamma}_2\rho_2\bar{\gamma}_0\rho_0 + \bar{\gamma}_2\rho_2) + \bar{\gamma}_0\rho_0 + 1}. \tag{7}$$

The decoding SINR of the weak signal for the strong user is given by

$$\gamma_{D\to C} = \frac{\alpha\bar{\gamma}_1\rho_1\left(\bar{\gamma}_0\rho_0+1\right)}{\left(1-\alpha\right)\left(\bar{\gamma}_1\rho_1\bar{\gamma}_0\rho_0+\bar{\gamma}_1\rho_1\right)+\bar{\gamma}_0\rho_0+1}. \quad (8)$$

Compared (7) with (8), it has $\gamma_{D\to C} > \gamma_{2,C}$, which indicates a perfect SIC can be conducted. Therefore, the SINR of the primary receiver is

$$\gamma_{2,D} = \frac{\left(1-\alpha\right)\bar{\gamma}_1\rho_1\bar{\gamma}_0\rho_0}{\left(1-\alpha\right)\bar{\gamma}_1\rho_1+\bar{\gamma}_0\rho_0+1}. \quad (9)$$

C. CHANNEL FADING MODELS

The hybrid satellite-terrestrial architecture has been incorporated in Digital Video Broadcast-Satellite Handheld (DVB-SH) standard using a geostationary (GEO) satellite at S (2-4 GHz) frequency band [28]. Therefore, the Shadowed-Rician fading model [6] is used for mobile/fixed receiver operating in various propagation environment for S-band in the paper. The probability density function (PDF) of $|H_{Si}|^2$ is shown as

$$f_{Si}\left(x\right) = \alpha_{Si}\exp\left(-\beta x\right){}_1F_1\left(m,1,\delta x\right), \quad (10)$$

where $i \in \{R,D\}$, ${}_1F_1\left(\cdot,\cdot,\cdot\right)$ denotes the confluent hypergeometric function and $\alpha_{Si} = \left(2bm\right)^m/2b\left(2bm+\Omega\right)^m$, $\delta = \Omega/2b\left(2bm+\Omega\right)$, and $\beta = 1/2b$, with $2b$ being the average power of the scatter component, Ω the average power of the line-of-sight (LOS) component, m is the Nakagami fading parameter, and $(\cdot)_k$ is the Pochhammer symbol. For simplicity, we suppose that m takes integer values, and rewrite Shadowed-Rician fading as

$$f_{Si}\left(x\right) = \alpha_{Si}\exp\left(\left(\delta-\beta\right)x\right)\sum_{k=0}^{m-1}\frac{\left(-1\right)^k\left(1-m\right)_k\left(\delta x\right)^k}{\left(k!\right)^2}. \quad (11)$$

The corresponding cumulative distribution function (CDF) can be obtained with the aid of [36, eq. 9.210.1], as

$$F_{Si}\left(x\right) = 1-\alpha_{Si}\exp\left(\left(\delta-\beta\right)x\right)\sum_{k=0}^{m-1}\frac{\left(-1\right)^k\left(1-m\right)_k}{k!}\times\sum_{p=0}^{k}\frac{\left(\delta-\beta\right)^{-(k+1-p)}x^p}{p!}e^{-(\delta-\beta)x}. \quad (12)$$

For terrestrial users, we consider Nakagami-m fading channels. For $j \in \{C,D\}$, the PDF of $\left|H_{Rj}\right|^2$ is given as

$$f_{Rj}\left(x\right) = \left(\frac{m_{Rj}}{\Omega_{Rj}}\right)^{m_{Rj}}\frac{x^{m_{Rj}-1}}{\Gamma\left(m_{Rj}\right)}e^{-\frac{m_{Rj}x}{\Omega_{Rj}}}, \quad (13)$$

where m_{Rj} is fading severity, which is assumed as integer values in this paper, Ω_{Rj} is average power, $\Gamma\left(\cdot\right)$ denotes the complete gamma function. The corresponding CDF can be obtained by

$$F_{Rj}\left(x\right) = \frac{1}{\Gamma\left(m_{Rj}\right)}\Upsilon\left(m_{Rj},\frac{m_{Rj}x}{\Omega_{Rj}}\right), \quad (14)$$

where $\Upsilon\left(\cdot\right)$ denotes lower incomplete gamma function.

III. THE OP PERFORMANCE ANALYSIS

In this section, we conduct the performance analysis of CHSTONs in the absence of a direct link between S and D.

A. THE EXACT OP EXPRESSIONS

The OP is defined as the probability that the instantaneous SINR γ_k falls below a predefined threshold γ_{th}, i.e.,

$$P_{out}\left(\gamma_{th}\right) = \Pr\left(\gamma_k < \gamma_{th}\right) = F_{\gamma_k}\left(\gamma_{th}\right), \quad (15)$$

where $F_{\gamma_k}\left(\cdot\right)$ denotes the CDF of γ_k.

Due to the property of NOMA, the instantaneous channel condition determines the power allocation and SIC implementation. In order to simplify equations, we adopt $m_1 = m_{RD}$, $m_2 = m_{RC}$, $\Omega_1 = \Omega_{RD}$, and $\Omega_2 = \Omega_{RC}$. Thus, the OP of AF protocols for the primary user can be given as

$$P_{out\_RD}\left(\gamma_{th}\right) = \Pr\left(\bar{\gamma}_1\rho_1 \le \bar{\gamma}_1\rho_1, \gamma_{1,D} < \gamma_{th}\right) + \Pr\left(\bar{\gamma}_1\rho_1 > \bar{\gamma}_1\rho_1, \gamma_{2,D} < \gamma_{th}\right). \quad (16)$$

When the primary user serves as the weak user, the OP can be calculated by (17), as shown at the bottom of this page, where $\varphi_1 = \gamma_{th}/[\bar{\gamma}_1\left(\alpha+\gamma_{th}\left(\alpha-1\right)\right)]$, and $\gamma_{th} < \alpha/(1-\alpha)$. Substituting (14) into (17) along with [36, (3.381.1)], we get

$$\kappa_1 = a_D\sum_{n=0}^{m_2-1}\frac{1}{n!}t^n v_1^{-n-m_1}\Upsilon\left(n+m_1, v_1\varphi_1\right), \quad (18)$$

where $v_C = m_2/\Omega_2$, $t = \bar{\gamma}_1/\bar{\gamma}_2$, $v_1 = tv_C + v_D$, and $a_D = \left(m_1/\Omega_1\right)^{m_1}\Gamma^{-1}\left(m_1\right)$.

In the derivation of κ_2, substitute (12) into (17), express $(x+\varphi)^n$ in terms of binomial expression with [36, (1.111)], utilize [36, (3.382.4, 3.471.9)], and then

$$\begin{aligned}&\Pr\left(\bar{\gamma}_1\rho_1 \le \bar{\gamma}_2\rho_2, \gamma_{1,D} < \gamma_{th}\right)\\ &= \int_0^{\varphi_1}\left[1-F_{RC}\left(tx\right)\right]f_{RD}\left(x\right)dx + \int_{\varphi_1}^{\infty}\left[1-F_{RC}\left(tx\right)\right]F_{SR}\left[\frac{\varphi\left(1+\bar{\gamma}_1x\right)}{\bar{\gamma}_0\left(x-\varphi_1\right)}\right]f_{RD}\left(x\right)dx\\ &= \underbrace{\int_0^{\varphi_1}\left[1-F_{RC}\left(tx\right)\right]f_{RD}\left(x\right)dx}_{\kappa_1} + \underbrace{\int_0^{\infty}\left[1-F_{RC}\left(t\left(x+\varphi_1\right)\right)\right]F_{SR}\left[\frac{1+\bar{\gamma}_1\left(x+\varphi_1\right)}{\varphi_1^{-1}\bar{\gamma}_0x}\right]f_{RD}\left(x+\varphi_1\right)dx}_{\kappa_2}, \end{aligned} \quad (17)$$

$$\kappa_2 = a_D e^{-v_1\varphi_1}\sum_{n=0}^{m_2-1}\frac{1}{n!}t^n\sum_{m=0}^{m_1+n-1}\binom{m_1+n-1}{m}\varphi_1^{m_1+n-1-m}v_1^{-m-1}\Gamma(m+1)$$
$$-\omega_1\sum_{n=0}^{m_2-1}\frac{t^n}{n!}\Xi_{k,p}\left(\frac{\varphi_1}{\bar{\gamma}_0}\right)^p\sum_{i=0}^{p}\binom{p}{i}\bar{\gamma}_1^i\sum_{l=0}^{n+i+m_1-1}\binom{i+m_1+n-1}{l}\varphi_1^{i+m_1+n-1-l}\left(\frac{v_2}{v_1}\right)^{\frac{l-p+1}{2}}K_{1+l-p}\left(2\sqrt{v_1v_2}\right). \quad (19)$$

$$\Pr\left(\bar{\gamma}_1\rho_1 > \bar{\gamma}_2\rho_2, \gamma_{2,D} < \gamma_{th}\right)$$
$$= \int_0^{\varphi_2} F_{RC}(tx) f_{RD}(x)\,dx + \int_{\varphi_2}^{\infty} F_{RC}(tx) F_{SR}\left[\frac{\varphi_2(1+(1-\alpha)\bar{\gamma}_1 x)}{\bar{\gamma}_0(x-\varphi_2)}\right] f_{RD}(x)dx$$
$$= \underbrace{\int_0^{\varphi_2} F_{RC}(tx) f_{RD}(x)\,dx}_{\kappa_3} + \underbrace{\int_0^{\infty} F_{RC}[t(x+\varphi_2)] F_{SR}\left[\frac{1+(1-\alpha)\bar{\gamma}_1(x+\varphi_2)}{\varphi_2^{-1}\bar{\gamma}_0 x}\right] f_{RD}(x+\varphi_2)dx}_{\kappa_4}, \quad (21)$$

$$\kappa_4$$
$$= 1 - F_{RD}(\varphi_2) - a_D e^{-v_1\varphi_2}\sum_{n=0}^{m_2-1}\frac{t^n}{n!}\sum_{m=0}^{m_1+n-1}\binom{m_1+n-1}{m}\varphi_2^{m_1+n-1-m}v_1^{-m-1}\Gamma(m+1)$$
$$-\omega_2\Xi_{k,p}\left(\frac{\varphi_2}{\bar{\gamma}_0}\right)^p\sum_{i=0}^{p}\binom{p}{i}(1-\alpha)^i\bar{\gamma}_1^i\sum_{l=0}^{i+m_1-1}\binom{i+m_1-1}{l}\varphi_2^{i+m_1-1-l}\left(\frac{v_3}{v_D}\right)^{\frac{l-p+1}{2}}K_{1+l-p}\left(2\sqrt{v_D v_3}\right)$$
$$+\omega_3\sum_{n=0}^{m_2-1}\frac{t^n}{n!}\Xi_{k,p}\left(\frac{\varphi_2}{\bar{\gamma}_0}\right)^p\sum_{i=0}^{p}\binom{p}{i}(1-\alpha)^i\bar{\gamma}_1^i\sum_{l=0}^{n+i+m_1-1}\binom{i+m_1+n-1}{l}\varphi_2^{i+m_1+n-1-l}\left(\frac{v_3}{v_1}\right)^{\frac{l-p+1}{2}}K_{1+l-p}\left(2\sqrt{v_1v_3}\right). \quad (23)$$

obtain the expression of κ_2 as (19), as shown at the top of this page, where $v_2 = \theta\varphi_1(1+\varphi_1\bar{\gamma}_1)/\bar{\gamma}_0$, $\omega_1 = 2a_D\exp\left(-v_1\varphi_1 - \theta\varphi_1\bar{\gamma}_1/\bar{\gamma}_0\right)$, $\theta = \beta_{SR} - \delta_{SR}$,

$$\Xi_{k,p}(\cdot) = \alpha_{SR}\sum_{k=0}^{m-1}\frac{(-1)^k(1-m_{SR})_k}{k!} \times\sum_{p=0}^{k}\frac{k!(\beta_{SR}-\delta_{SR})^{-(k+1-p)}}{p!}(\cdot), \quad (20)$$

and $K_V(Z)$ is the modified Bessel function of second kind. In another case (i.e. the primary is the weak user), the OP can be obtained by (21), as shown at the top of this page, where $\varphi_2 = \gamma_{th}/(\bar{\gamma}_1 - \alpha\bar{\gamma}_1)$. The κ_3 and κ_4 are obtained in the same way. Therefore,

$$\kappa_3 = F_{RD}(\varphi_2) - a_D\sum_{n=0}^{m_2-1}\frac{1}{n!}t^n v_1^{-n-m_1}\Upsilon(n+m_1, v_1\varphi_2), \quad (22)$$

and κ_4 is formulated as (23), as shown at the top of this page, where $\omega_2 = 2a_D\exp(-v_D\varphi_2)\exp\left(-\theta\varphi_2(1-\alpha)\bar{\gamma}_1/\bar{\gamma}_0\right)$, $v_3 = \theta\varphi_2[1+(1-\alpha)\bar{\gamma}_1\varphi_2]/\bar{\gamma}_0$, and $\omega_3 = 2a_D\exp\left(-v_1\varphi_2 - \theta\varphi_2(1-\alpha)\bar{\gamma}_1/\bar{\gamma}_0\right)$.

The OP for secondary user in AF protocols can be given by

$$P_{out\_RC}(\gamma_{th}) = \Pr\left(\bar{\gamma}_1\rho_1 \le \bar{\gamma}_2\rho_2, \gamma_{2,C} < \gamma_{th}\right) + \Pr\left(\bar{\gamma}_1\rho_1 > \bar{\gamma}_2\rho_2, \gamma_{1,C} < \gamma_{th}\right). \quad (24)$$

In order to get closed-form expression of the OP when the secondary user is the strong user, we assume $\gamma_{th} > (1-\alpha)/\alpha$, which is reasonable for demodulation and decoding. Consequently, the OP can be derived as (25), as shown at the top of the next page, where $\varphi_3 = \gamma_{th}/(\bar{\gamma}_2 - \alpha\bar{\gamma}_2)$. The κ_5 is

$$\kappa_5 = F_{RC}(\varphi_3) - a_C\sum_{n=0}^{m_1-1}\frac{t^{-n}}{n!}v_4^{-n-m_2}\Upsilon(n+m_2, v_4\varphi_3), \quad (26)$$

where $v_4 = v_D/t + v_C$, $a_C = \left(m_2/\Omega_2\right)^{m_2}\Gamma^{-1}(m_2)$. κ_5 is formulated as (27), as shown at the top of the next page, where $v_5 = \theta\alpha\varphi_3^2\bar{\gamma}_2/\bar{\gamma}_0$, $\omega_4 = 2a_C\exp\left(-v_C\varphi_3 - \theta(\alpha\varphi_3\bar{\gamma}_2 - 1)/\bar{\gamma}_0\right)$, and $\omega_5 = 2a_C\exp\left(-v_4\varphi_3 - \theta(\alpha\varphi_3\bar{\gamma}_2 - 1)/\bar{\gamma}_0\right)$. When the secondary user is the weak user, the OP can be obtain by (28), as shown at the top of the next page, where $\varphi_4 = \gamma_{th}/[\alpha\bar{\gamma}_2 - (1-\alpha)\gamma_{th}\bar{\gamma}_2]$.

B. THE ASYMPTOTIC OP EXPRESSIONS

To evaluate the achievable diversity orders and coding gains of each user in the considered CHSTONs, we investigate the asymptotic OP performance at the high SINR in this subsection.

Th approximated CDF of satellite link [23] is denoted as

$$F_{SR}(u) \approx \alpha_{SR}\sum_{k=0}^{+\infty}\frac{(m_{SR})_k\delta_{SR}^k}{\beta_{SR}^{k+1}}\frac{\beta_{SR}^{k+1}u^{k+1}}{k+1} \approx \alpha_{SR}u. \quad (29)$$

The approximated PDF of terrestrial links can be given by

$$f_{\rho_{Rj}}(x) = \left(\frac{m_{Rj}}{\Omega_{Rj}}\right)^{m_{Rj}}\frac{x^{m_{Rj}-1}}{\Gamma\left(m_{Rj}\right)}. \quad (30)$$

$$\begin{aligned}
&\Pr\left(\bar{\gamma}_1\rho_1 \le \bar{\gamma}_2\rho_2, \gamma_{1,C} < \gamma_{th}\right) \\
&= \int_0^{\varphi_3} F_{RD}\left(xt^{-1}\right) f_{RC}(x)\, dx + \int_{\varphi_3}^{\infty} F_{RD}(tx)\, F_{SR}\left[\frac{\varphi_3\left(1+\left(\alpha-\varphi_3^{-1}\right)\bar{\gamma}_2 x\right)}{\bar{\gamma}_0(x-\varphi_3)}\right] f_{RC}(x)dx \\
&= \underbrace{\int_0^{\varphi_3} F_{RD}\left(xt^{-1}\right) f_{RC}(x)\, dx}_{\kappa_5} + \underbrace{\int_0^{\infty} F_{RD}\left[t^{-1}(x+\varphi_3)\right] F_{SR}\left[\frac{1+\left(\alpha\bar{\gamma}_2-\varphi_3^{-1}\right)(x+\varphi_3)}{\varphi_3^{-1}\bar{\gamma}_0 x}\right] f_{RC}(x+\varphi_3)dx}_{\kappa_6}, \qquad (25)
\end{aligned}$$

$$\begin{aligned}
\kappa_6 &= 1 - F_{RC}(\varphi_3) - a_C e^{-v_4\varphi_3} \sum_{n=0}^{m_{RD}-1} \frac{t^{-n}}{n!} \sum_{m=0}^{m_{RC}+n-1} \binom{m_{RC}+n-1}{m} \varphi_3^{m_{RC}+n-1-m} v_4^{-m-1}\Gamma(m+1) \\
&\quad - \omega_4 \Xi_{k,p}\left(\frac{\varphi_3}{\bar{\gamma}_0}\right)^p \sum_{i=0}^{p}\binom{p}{i}\left(\alpha\bar{\gamma}_2-\varphi_3^{-1}\right)^i \sum_{l=0}^{i+m_2-1}\binom{i+m_2-1}{l}\varphi_3^{i+m_2-1-l}\left(\frac{v_5}{v_C}\right)^{\frac{l-p+1}{2}} K_{1+l-p}\left(2\sqrt{v_C v_5}\right) \\
&\quad + \omega_5 \sum_{n=0}^{m_{1-1}} \frac{t^{-n}}{n!}\Xi_{k,p}\left(\frac{\varphi_3}{\bar{\gamma}_0}\right)^p \sum_{i=0}^{p}\binom{p}{i}\left(\alpha\bar{\gamma}_2-\varphi_3^{-1}\right)^i \sum_{l=0}^{n+i+m_2-1}\binom{i+m_2+n-1}{l}\varphi_3^{i+m_2+n-1-l}\left(\frac{v_5}{v_4}\right)^{\frac{l-p+1}{2}} K_{1+l-p}\left(2\sqrt{v_4 v_5}\right). \qquad (27)
\end{aligned}$$

$$\begin{aligned}
&\Pr\left(\bar{\gamma}_1\rho_1 > \bar{\gamma}_2\rho_2, \gamma_{2,C} < \gamma_{th}\right) \\
&= \int_0^{\varphi_4} [1 - F_{RD}(x/t)] f_{RC}(x)\, dx = a_C \sum_{n=0}^{m_{1-1}} \frac{1}{n!} t^{-n} v_4^{-n-m_2} \Upsilon(n+m_2, v_4\varphi_4). \qquad (28)
\end{aligned}$$

Then, the corresponding CDF can be expressed as

$$F_{\rho_{Rj}}(x) = \left(\frac{m_{Rj}}{\Omega_{Rj}}\right)^{m_{Rj}} \frac{x^{m_{Rj}}}{\Gamma\left(m_{Rj}+1\right)}. \qquad (31)$$

To be noticed, the fading severity m does not require to be an integer in approximated expressions. Based on approximated CDF, the asymptotic OP expressions for each user are obtained as follows.

For the primary user, the SINR can be obtained from (4) and (9). The SINR tend to infinity means the transmitted power tend to infinity, i.e., $\bar{\gamma}_0 \to \infty$ or $\bar{\gamma}_1 \& \bar{\gamma}_2 \to \infty$. Thus, the approximate of γ_D is

$$\begin{aligned}
\gamma_D = &\min\left(\frac{\alpha\bar{\gamma}_0\rho_0}{(1-\alpha)\bar{\gamma}_0\rho_0+1}, \frac{\alpha\bar{\gamma}_1\rho_1}{(1-\alpha)\bar{\gamma}_1\rho_1+1}\right)\Big|_{\bar{\gamma}_1\rho_1\le\bar{\gamma}_2\rho_2} \\
&+\min\left((1-\alpha)\bar{\gamma}_1\rho_1, \bar{\gamma}_0\rho_0\right)\Big|_{\bar{\gamma}_1\rho_1>\bar{\gamma}_2\rho_2}. \qquad (32)
\end{aligned}$$

Furthermore, the asymptotic OP of the primary user can be obtained by (33), as shown at the bottom of the next page, where $\bar{\gamma}_0 = \eta_0\bar{\gamma}$, $\bar{\gamma}_1 = \eta_1\bar{\gamma}$ and $\bar{\gamma}_2 = \eta_2\bar{\gamma}$. It is obvious that the diversity order is $G_1^d = \min(1, m_1)$ and the code gain is $G_1^c = {C_D}^{-1/G_1^d} \Big/ \gamma_{th}$, with

$$C_D = \begin{cases} \dfrac{\alpha_{SR}}{\eta_0(\alpha-(1-\alpha)\gamma_{th})} + \dfrac{\alpha_{SR}}{\eta_0} & m_1 > 1 \\ \dfrac{\alpha_{SR}/\eta_0 + v_D/\eta_1}{\alpha-(1-\alpha)\gamma_{th}} + \dfrac{\alpha_{SR}}{\eta_0} & m_1 = 1 \\ \dfrac{1}{\Gamma(m_1+1)}\left(\dfrac{v_D}{\eta_1(\alpha-(1-\alpha)\gamma_{th})}\right)^{m_1} & m_1 < 1. \end{cases} \qquad (34)$$

For secondary user, the SINR can be obtained from (6) and (7). Therefore, the approximate of γ_C is

$$\begin{aligned}
\gamma_C = &\min\left((1-\alpha)(\bar{\gamma}_0\rho_0+1), (1-\alpha)\bar{\gamma}_2\rho_2\right)\Big|_{\bar{\gamma}_1\rho_1\le\bar{\gamma}_2\rho_2} \\
&+\alpha(\bar{\gamma}_0\rho_0+1)\Big/((1-\alpha)\bar{\gamma}_0\rho_0+1)\Big|_{\bar{\gamma}_1\rho_1>\bar{\gamma}_2\rho_2}. \qquad (35)
\end{aligned}$$

Further, the asymptotic OP of the secondary user is shown as (36), as shown at the bottom of the next page. One can straightforwardly find that the diversity order is $G_2^d = \min(1, m_2)$ and code gain is $G_2^c = {C_C}^{-1/G_2^d} \Big/ \gamma_{th}$ with

$$C_C = \begin{cases} \dfrac{\alpha_{SR}}{\eta_0\gamma_{th}}\dfrac{\alpha\gamma_{th}-1+\alpha}{(1-\alpha)} & m_2 > 1 \\ \dfrac{\alpha_{SR}}{\eta_0\gamma_{th}}\dfrac{\alpha\gamma_{th}-1+\alpha}{(1-\alpha)} + \dfrac{(1-\alpha)v_C}{\eta_2(\alpha-(1-\alpha)\gamma_{th})} & m_2 = 1 \\ \dfrac{1}{\Gamma(m_2+1)}\left(\dfrac{(1-\alpha)v_C}{\eta_2(\alpha-(1-\alpha)\gamma_{th})}\right)^{m_2} & m_2 < 1. \end{cases} \qquad (37)$$

IV. SIMULATION RESULTS

In this section, representative simulation results are presented to validate the theoretical results and quantify the impact of various system parameters on the performance of the considered network. All simulation results are obtained with 10^7 channel realizations. According to the actual measurement, the typical satellite channel parameters of different shadowing are listed in Table 1 [6].

Fig. 2 reveals the OP of the primary user for different $\bar{\gamma}_0 = \bar{\gamma}_1 = \bar{\gamma}_2 = \bar{\gamma}$, i.e., $\eta_0 = \eta_1 = \eta_2$, where the

TABLE 1. Satellite channel parameters.

Parameters	b	m	Ω
Frequent heavy shadowing	0.063	1	8.97×10^{-4}
Average shadowing	0.126	10	0.835
Infrequent light shadowing	0.158	20	1.29

first temporal phase link undergoes infrequent light shadowing (ILS) and average shadowing (AS). We assume the DC link undergoes frequent heavy shadowing for the purpose of comparison. The second temporal phase link channel coefficients are $m_1 = m_2 = 2, \Omega_1 = \Omega_2 = 1$. The decode threshold is set as $\gamma_{th} = 1$dB and the NOMA power split factor $\alpha = 0.7$. Those Monte Carlo simulation OP curves excellently agree with analytical results across the entire average SNR range, and asymptotic curves agree with analytical and simulation results at the regime of high SNR. Comparing with the scenario of the DC link, the OP of the primary user is significantly reduced by adopting the overlay relay with the NOMA scheme, which means that the overlay relay enhance the reliability of the transmission. The parallel asymptotic OP curves indicate that the same diversity orders and varying code gains. Owing to the slighter shadowing of the first temporal phase, the OP performance of ILS is better than that of AS, which indicates that we could choose the relay with the best channel quality, if there is a multi-relay scenario. In addition, comparing OP performance of NOMA scheme with TDMA, it proclaims that the NOMA scheme achieves higher resource utilization with the same amount of transmitting power.

Fig. 3 illustrates the OP of the primary user for different average SNR, where the satellite link undergoes ILS and the second temporal phase link undergoes two kind fading scenarios. The first scenario channel coefficients are $m_1 = 0.5, m_2 = 0.5, \Omega_1 = \Omega_2 = 1$. The analytical curve is calculated directly by OP definition in this scenario due to the non-integer value of m_1 and m_2, which is calculated by the integral calculation in MATLAB software. The second scenario channel coefficients are $m_1 = 2, m_2 = 2, \Omega_1 = \Omega_2 = 1$. The analytical curve can be calculated by the close-form expression in this scenario. The decode threshold is set as $\gamma_{th} = 1$dB and the NOMA power split factor $\alpha = 0.7$. It is obvious to find out the NOMA scheme is superior of the OMA scheme. According to the diverse gradient of asymptotic OP curves, the achievable diversity orders are different, which are closely related to the value of second link channel parameter m_1. When $m_1 = 0.5$ and $m_1 = 2$, diversity order is 0.5 and 1 respectively.

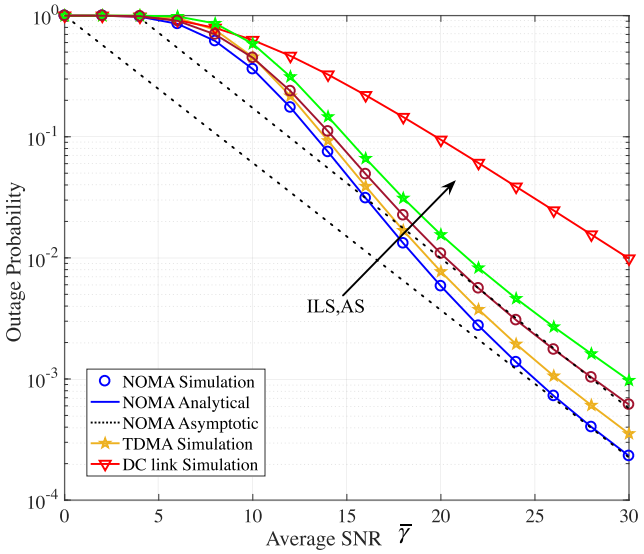

FIGURE 2. The outage probability versus average SNR $\bar{\gamma}$ of the primary user for different shadowing in the first temporal phase.

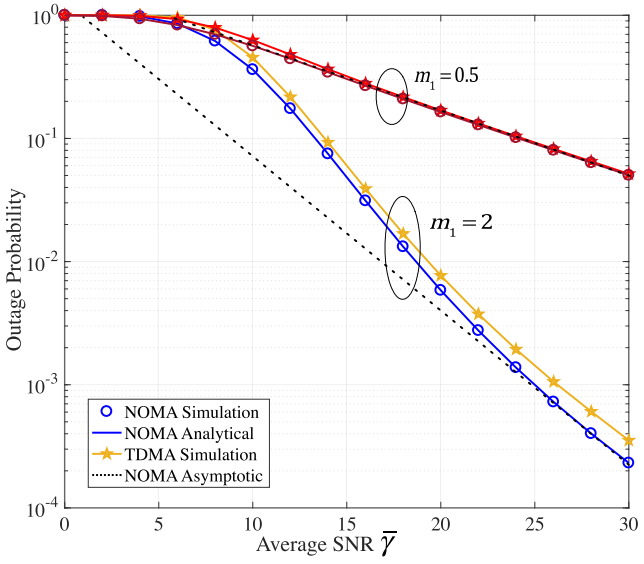

FIGURE 3. The outage probability versus average SNR $\bar{\gamma}$ of the primary user for different fading in the second temporal phase.

Fig. 4 depicts the OP of the secondary user for different average SNR, where the satellite link undergoes ILS and AS for comparison, and the second temporal phase link channel coefficients are $m_1 = m_2 = 2, \Omega_1 = \Omega_2 = 1$. The decode threshold is set as $\gamma_{th} = 1$dB and the NOMA power split factor $\alpha = 0.7$. Due to the AF protocols of the cognitive

$$P^{\infty}_{out\_RD}(\gamma_{th}) \approx \frac{\alpha_{SR}\gamma_{th}}{\eta_0\bar{\gamma}(\alpha-(1-\alpha)\gamma_{th})} + \frac{1}{\Gamma(m_1+1)}\left(\frac{v_1\gamma_{th}}{\eta_1\bar{\gamma}(\alpha-(1-\alpha)\gamma_{th})}\right)^{m_1} + \frac{\alpha_{SR}\gamma_{th}}{\eta_0\bar{\gamma}}, \tag{33}$$

$$P^{\infty}_{out\_RC}(\gamma_{th}) \approx \alpha_{SR}\frac{\alpha\gamma_{th}-1+\alpha}{(1-\alpha)\eta_0\bar{\gamma}} + \frac{1}{\Gamma(m_2+1)}\left(\frac{(1-\alpha)v_C\gamma_{th}}{\eta_2\bar{\gamma}(\alpha-(1-\alpha)\gamma_{th})}\right)^{m_2}. \tag{36}$$

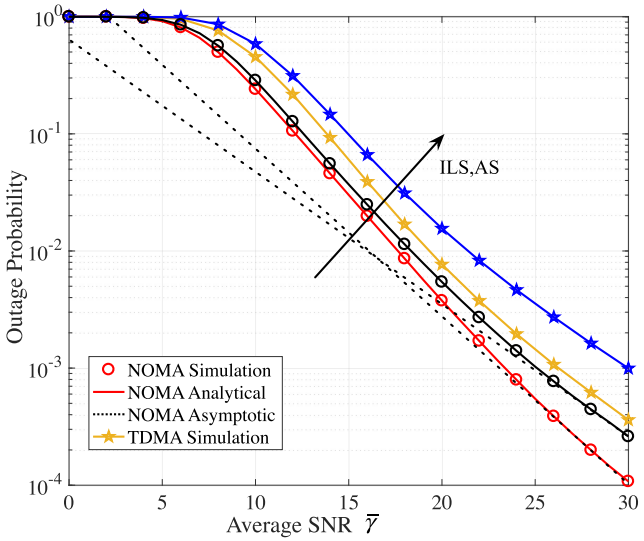

FIGURE 4. The outage probability versus average SNR $\bar{\gamma}$ of the secondary user for different shadowing in the first temporal phase.

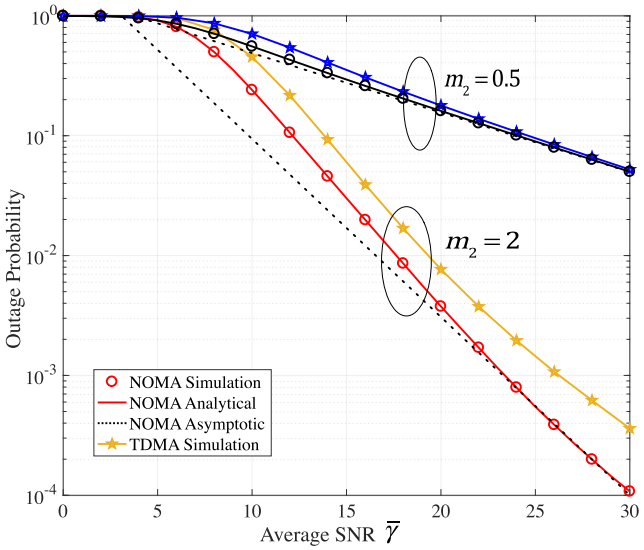

FIGURE 5. The outage probability versus average SNR $\bar{\gamma}$ of the secondary user for different fading in the second temporal phase.

relay, the amplified noise from the first temporal phase would deteriorate the performance of the secondary user. Since the NOMA power allocation profile is determined by the instantaneous block fading channel, comparing Fig. 2 and Fig. 4, the OP performance of the primary and secondary user is almost the same (i.e., on the same order of magnitude), which indicates the fairness of NOMA scheme in CHSTONs. Fig.5 is given to express the diversity orders of the secondary user, where the parameter settings are the same as in Fig. 3.

The influence of the power split factor α on the system performance is shown in Fig. 6, where the first temporal phase is assumed to be ILS for both the primary and the secondary users, and the second temporal phase link channel coefficients are $m_1 = m_2 = 2, \Omega_1 = \Omega_2 = 1$. The decode

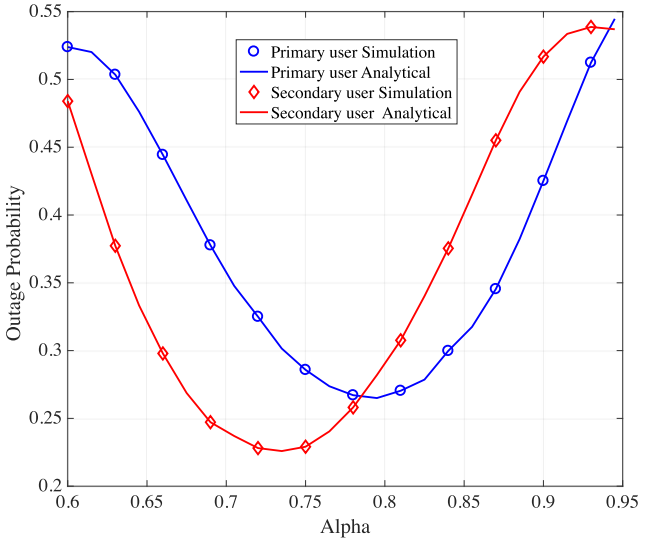

FIGURE 6. The outage probability versus power split factor α for both the primary user and the secondary user.

threshold is set as $\gamma_{th} = 1$dB. As we see, the optimal NOMA split factor is distinguished for two users. When $\alpha = 0.7$ as a verification, the performance of secondary is more reliable than the primary user, which can be derived from Fig. 2 versus Fig. 4 and Fig. 3 versus Fig. 5. In order to improve the performance and fairness for two users, the NOMA split factor α is suggested to set between 0.72 and 0.8 when $\gamma_{th} = 1$dB. In addition, the optimal α would be adjusted for the various threshold accordingly.

V. CONCLUSION

In this paper, a NOMA scheme for CHSTONs is proposed to tackle the fairness issue and improve the spectral efficiency. The NOMA power allocation strategy is modified by instantaneous channel conditions to make the weak user obtain more power than the strong user, which resolves the fairness of overlay paradigm. The closed-form and asymptotic OP expressions are derived for the primary user and secondary user, respectively. In addition, we introduce the superiority of the NOMA scheme and the effect of key parameters on the performance of networks. To fully explore the superiority of combination NOMA with CHSTONs, multi-users scheduling and relays selection would be studied for different fading severity in our future work.

REFERENCES

[1] P. K. Upadhyay and P. K. Sharma, "Max-max user-relay selection scheme in multiuser and multirelay hybrid satellite-terrestrial relay systems," *IEEE Commun. Lett.*, vol. 20, no. 2, pp. 268–271, Feb. 2016.

[2] W. Lu, K. An, and T. Liang, "Robust beamforming design for sum secrecy rate maximization in multibeam satellite systems," *IEEE Trans. Aerosp. Electron. Syst.*, vol. 55, no. 3, pp. 1568–1572, Jun. 2019.

[3] M. R. Bhatnagar and M. K. Arti, "Performance analysis of AF based hybrid satellite-terrestrial cooperative network over generalized fading channels," *IEEE Commun. Lett.*, vol. 17, no. 10, pp. 1912–1915, Oct. 2013.

[4] M. K. Arti and V. Jain, "Relay selection-based hybrid satellite-terrestrial communication systems," *IET Commun.*, vol. 11, no. 17, pp. 2566–2574, Nov. 2017.

[5] X. Liang, J. Jiao, S. Wu, and Q. Zhang, "Outage analysis of multirelay multiuser hybrid satellite-terrestrial millimeter-wave networks," *IEEE Wireless Commun. Lett.*, vol. 7, no. 6, pp. 1046–1049, Dec. 2018.
[6] K. An, T. Liang, G. Zheng, X. Yan, Y. Li, and S. Chatzinotas, "Performance limits of cognitive uplink FSS and terrestrial FS for Ka-band," *IEEE Trans. Aerosp. Electron. Syst.*, to be published. doi: 10.1109/TAES.2018.2886611.
[7] K. Guo, K. An, B. Zhang, Y. Huang, and G. Zheng, "Outage analysis of cognitive hybrid satellite-terrestrial networks with hardware impairments and multi-primary users," *IEEE Wireless Commun. Lett.*, vol. 7, no. 5, pp. 816–819, Oct. 2018.
[8] V. Singh, S. Solanki, and P. K. Upadhyay, "Cognitive relaying cooperation in satellite-terrestrial systems with multiuser diversity," *IEEE Access*, vol. 6, pp. 65539–65547, 2018.
[9] W. Liang, S. X. Ng, and L. Hanzo, "Cooperative overlay spectrum access in cognitive radio networks," *IEEE Commun. Surveys Tuts.*, vol. 19, no. 3, pp. 1924–1944, 3rd Quart., 2017.
[10] P. K. Sharma, P. K. Upadhyay, D. B. da Costa, P. S. Bithas, and A. G. Kanatas, "Performance analysis of overlay spectrum sharing in hybrid satellite-terrestrial systems with secondary network selection," *IEEE Trans. Wireless Commun.*, vol. 16, no. 10, pp. 6586–6601, Oct. 2017.
[11] Y. Liu, Z. Qin, M. Elkashlan, Z. Ding, A. Nallanathan, and L. Hanzo, "Nonorthogonal multiple access for 5G and beyond," *Proc. IEEE*, vol. 105, no. 12, pp. 2347–2381, Dec. 2017.
[12] Z. Ding, P. Fan, and H. V. Poor, "Impact of user pairing on 5G nonorthogonal multiple-access downlink transmissions," *IEEE Trans. Veh. Technol.*, vol. 65, no. 8, pp. 6010–6023, Aug. 2016.
[13] Z. Ding, H. Dai, and H. V. Poor, "Relay selection for cooperative NOMA," *IEEE Wireless Commun. Lett.*, vol. 5, no. 4, pp. 416–419, Aug. 2016.
[14] S. M. R. Islam, N. Avazov, O. A. Dobre, and K.-S. Kwak, "Power-domain non-orthogonal multiple access (NOMA) in 5G systems: Potentials and challenges," *IEEE Commun. Surveys Tuts.*, vol. 19, no. 2, pp. 721–742, 2nd Quart., 2017.
[15] O. Abbasi, A. Ebrahimi, and N. Mokari, "NOMA inspired cooperative relaying system using an AF relay," *IEEE Wireless Commun. Lett.*, vol. 8, no. 1, pp. 261–264, Feb. 2019.
[16] J. A. Oviedo and H. R. Sadjadpour, "A fair power allocation approach to NOMA in multiuser SISO systems," *IEEE Trans. Veh. Technol.*, vol. 66, no. 9, pp. 7974–7985, Sep. 2017.
[17] M. Caus, M. Á. Vázquez, and A. Pérez-Neira, "NOMA and interference limited satellite scenarios," in *Proc. 50th Asilomar Conf. Signals, Syst. Comput.*, Pacific Grove, CA, USA, Nov. 2016, pp. 497–501.
[18] R. Wan, L. Zhu, T. Li, and L. Bai, "A NOMA-PSO based cooperative transmission method in satellite communication systems," in *Proc. IEEE WCSP*, Nanjing, China, Oct. 2017, pp. 1–6.
[19] X. Yan, K. An, T. Liang, G. Zheng, Z. Ding, S. Chatzinotas, and Y. Liu, "The application of power-domain non-orthogonal multiple access in satellite communication networks," *IEEE Access*, vol. 7, pp. 63531–63539, 2019.
[20] X. Yan, H. Xiao, C.-X. Wang, K. An, A. T. Chronopoulos, and G. Zheng, "Performance analysis of NOMA-Based land mobile satellite networks," *IEEE Access*, vol. 6, pp. 31327–31339, 2018.
[21] N. A. K. Beigi and M. R. Soleymani, "Interference management using cooperative NOMA in multi-beam satellite systems," in *Proc. ICC*, Kansas City, MO, USA, May 2018, pp. 1–6.
[22] T. Qi, W. Feng, and Y. Wang, "Outage performance of non-orthogonal multiple access based unmanned aerial vehicles satellite networks," *China Commu.*, vol. 15, no. 5, pp. 1–8, May 2018.
[23] X. Zhu, C. Jiang, L. Kuang, N. Ge, and J. Lu, "Non-orthogonal multiple access based integrated terrestrial-satellite networks," *IEEE J. Sel. Areas Commun.*, vol. 35, no. 10, pp. 2253–2267, Oct. 2017.
[24] Z. Lin, M. Lin, J.-B. Wang, T. de Cola, and J. Wang, "Joint beamforming and power allocation for satellite-terrestrial integrated networks with non-orthogonal multiple access," *IEEE J. Sel. Areas Commun.*, vol. 13, no. 3, pp. 657–670, Jun. 2019.
[25] X. Yan, H. Xiao, K. An, G. Zheng, and W. Tao, "Hybrid satellite terrestrial relay networks with cooperative non-orthogonal multiple access," *IEEE Commun. Lett.*, vol. 22, no. 5, pp. 978–981, May 2018.
[26] X. Yan, H. Xiao, K. An, and C.-X. Wang, "Outage performance of NOMA-based hybrid satellite-terrestrial relay networks," *IEEE Wireless Commun. Lett.*, vol. 7, no. 4, pp. 538–541, Aug. 2018.
[27] L. Lv, J. Chen, Q. Ni, Z. Ding, and H. Jiang, "Cognitive non-orthogonal multiple access with cooperative relaying: A new wireless frontier for 5G spectrum sharing," *IEEE Commun. Mag.*, vol. 56, no. 4, pp. 188–195, Apr. 2018.
[28] L. Lv, Q. Ni, Z. Ding, and J. Chen, "Application of non-orthogonal multiple access in cooperative spectrum-sharing networks over Nakagami-*m* fading channels," *IEEE Trans. Veh. Technol.*, vol. 66, no. 6, pp. 5506–5511, Jun. 2017.
[29] L. Lv, L. Yang, H. Jiang, T. H. Luan, and J. Chen, "When NOMA meets multiuser cognitive radio: Opportunistic cooperation and user scheduling," *IEEE Trans. Veh. Technol.*, vol. 67, no. 7, pp. 6679–6684, Jul. 2018.
[30] L. Lv, J. Chen, Q. Ni and Z. Ding, "Design of cooperative non-orthogonal multicast cognitive multiple access for 5G systems: User scheduling and performance analysis," *IEEE Trans. Commun.*, vol. 65, no. 6, pp. 2641–2656, Jun. 2017.
[31] K. David and H. Berndt, "6G vision and requirements: Is there any need for beyond 5G?" *IEEE Veh. Technol. Mag.*, vol. 13, no. 3, pp. 72–80, Sep. 2018.
[32] *Digital Video Broadcasting (DVB): Framing Structure, Channel Coding and Modulation for Satellite Transmission to Handheld (DVB-SH)*, document ETSI EN 302 583 V1.0.0, Jun. 2007.
[33] S. A. Wilkus, J. D. Bailey, D. G. Brown, R. Dave, R. L. Dorn, J.-M. Hanriot, M. Hoffman, A. Kulkarni, C. S. Lee, L. R. Meader, J. M. Polakovic, and J. Sullivan, "Field measurements of a hybrid DVB-SH single frequency network with an inclined satellite orbit," *IEEE Trans. Broadcast.*, vol. 56, no. 4, pp. 523–531, Dec. 2010.
[34] L. Giupponi and C. Ibars, "Distributed cooperation in cognitive radio networks: Overlay versus underlay paradigm," in *Proc. IEEE 69th Veh. Technol. Conf. (VTC Spring)*, Barcelona, Spain, Apr. 2009, pp. 1–6.
[35] J. Perez-Romero, O. Sallent, R. Agusti, and L. Giupponi, "A novel on-demand cognitive pilot channel enabling dynamic spectrum allocation," in *Proc. 2nd IEEE Int. Symp. New Frontiers Dyn. Spectr. Access Netw.*, Dublin, Ireland, Apr. 2007, pp. 46–54.
[36] I. S. Gradshteyn and I. M. Ryzhik, *Table of Integrals, Series, and Products*, 7th ed. New York, NY, USA: Academic, 2007.

XIAOKAI ZHANG received the B.S. degree from the Harbin Institute of Technology (HIT), Harbin, China, in 2015, and the M.S. degree from PLA Army Engineering University, Nanjing, China, in 2017, where he is currently pursuing the Ph.D. degree. His research interests include satellite communications, polarization shift keying, physical-layer security, non-orthogonal multiple access (NOMA), cognitive radio, and reinforcement learning.

BANGNING ZHANG received the B.S. and M.S. degrees from the Institute of Communications Engineering (ICE), Nanjing, China, in 1984 and 1987, respectively. He is currently a Full Professor and the Head of the College of Communications Engineering, PLA Army Engineering University. He has authored or coauthored more than 80 conference and journal papers and has been granted over 20 patents in his research areas. His current research interests include communication anti-jamming technologies, microwave technologies, polarization technologies, satellite communications systems, cooperative communications, and physical-layer security. He has served as a Reviewer for several journals in communication field.

KANG AN received the B.E. degree in electronic engineering from the Nanjing University of Aeronautics and Astronautics, Nanjing, China, in 2011, the M.E. degree in communication engineering from the PLA University of Science and Technology, Nanjing, in 2014, and the Ph.D. degree in communication engineering from PLA Army Engineering University, Nanjing, in 2017. Since 2018, he has been with the National University of Defense Technology, Nanjing, where he is currently an Engineer. His current research interests include satellite communication, 5G mobile communication networks, and cognitive radio.

ZHUYUN CHEN received the B.S. degree from the School of Electronic and Information Engineering, South China University of Technology, Guangzhou, China, in 2014, and the M.S. degree from the College of Communications Engineering, PLA University of Science and Technology, Nanjing, China, in 2017. He is currently pursuing the Ph.D. degree in information and communication engineering with PLA Army Engineering University, Nanjing. His research interests include hybrid terrestrial-satellite communications, cognitive networks, game theory, and optimization techniques.

SILIN XIE received the B.S. degree from Tsinghua University, Beijing, China, in 2013, and the M.S. degree from the PLA University of Science and Technology, Nanjing, China, in 2016. He is currently pursuing the Ph.D. degree with PLA Army Engineering University, Nanjing. His research interests include satellite communication, non-orthogonal multiple access cooperative relay networks, and multiuser communication systems.

HENG WANG received the B.S. degree in electronic information science and technology from the China University of Mining and Technology (CUMT), in 2005, and the M.S. degree in information and signal processing from the Nanjing University of Science and Technology, in 2007. She is currently pursuing the Ph.D. degree in communications and information system with the College of Communications Engineering, PLA Army Engineering University, where she is also a Lecturer. Her research interests mainly include satellite communication, and signal design and detection.

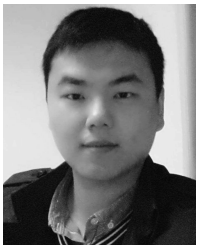

LONG WANG received the B.E. degree from the PLA University of Science and Technology, Nanjing, China, in 2011, and the M.E. degree from the PLA Army Academy of Artillery and Air Defense, Hefei, China, in 2014. He is currently with the Sixty-Third Research Institute, National University of Defense Technology, Nanjing. His research interests include digital communication and military communication.

DAOXING GUO received the B.S., M.S., and Ph.D. degrees from the College of Communications Engineering, PLA Army Engineering University, Nanjing, China, in 1995, 1999, and 2002, respectively, where he is currently a Full Professor and a Ph.D. Supervisor. He has authored or coauthored more than 40 conference and journal papers. His current research interests include satellite communications systems and transmission technologies, communication anti-jamming technologies, and communication anti-interception technologies, including physical-layer security. He holds over 20 patents in his research areas. He has served as a Reviewer for several journals in communication field.